Multiple scattering suppression in static light scattering by cross-correlation spectroscopy

A. Moussaïd and P. N. Pusey
Department of Physics and Astronomy, The University of Edinburgh, Mayfield Road, Edinburgh EH9 3JZ, Scotland
(Received 27 April 1999)

Cross-correlation techniques have been used successfully to suppress multiple scattering in dynamic light-scattering experiments on turbid samples. This allows dynamic information to be obtained straightfowardly by processing the remaining single scattering. Here we show that cross-correlation techniques can also be used to suppress multiple scattering in *static* light-scattering measurements. We use the two-color dynamic light-scattering method and exploit the fact that the amplitude of the time-dependent part of the measured intensity cross-correlation function depends on the ratio of the single-scattered intensity to the total (single + multiple) scattered intensity. The method is illustrated by measurements of the static structure factors of concentrated suspensions of ''hard-sphere'' colloids. Good agreement is found with those calculated in the Percus-Yevick approximation. [S1063-651X(99)15310-8]

PACS number(s): 82.70.Dd, 61.20.−p, 61.18.−j

I. INTRODUCTION

Light scattering is a powerful probe of complex fluids such as colloidal suspensions and solutions of polymers or amphiphiles. Static light scattering (SLS), in which the average scattered intensity is measured as a function of scattering angle, provides information on a sample's average structure. Dynamic light scattering (DLS) analyzes temporal fluctuations in the scattered light and provides information on a sample's dynamics, typically Brownian motions. There is a direct and relatively simple relationship between the properties of the material and the intensity and temporal fluctuations of *single*-scattered light. Multiple scattering, however, where a significant fraction of the incident photons is scattered twice or more on passing through the sample, complicates data analysis greatly. Thus there is strong motivation to develop methods to suppress multiple scattering so that interpretable light-scattering data can be obtained from optically turbid samples. Following the pioneering work of Phillies [1] in 1981, several schemes for multiple-scattering suppression have been developed. Until recently the emphasis has been on implementing these schemes in *dynamic* light scattering. Here we show how the methods can be adapted to *static* light scattering, allowing the determination of structural information from turbid samples. We illustrate this by measuring accurate static structure factors of concentrated suspensions of hard-sphere colloids (see [2] for a preliminary report and [3] for another application of the method).

Ordinary light scattering, both static and dynamic, uses one illuminating laser beam and one detector. The scattering geometry defines a scattering vector $\vec{Q}$, the difference between the propagation vectors of the incident and scattered light, which has magnitude

$$Q = \frac{4\pi}{\lambda}\sin\left(\frac{\theta}{2}\right), \tag{1}$$

where λ is the wavelength of the light in the sample and θ is the scattering angle. Singly scattered light probes the amplitude and time evolution of a single spatial Fourier component of the refractive-index fluctuations of the medium — frequently directly related to the density fluctuations — of wave vector $\vec{Q}$. A common feature of most multiple-scattering suppression schemes [4] is the use of *two* illuminating beams and *two* detectors whose outputs are cross correlated. The optics are arranged such that each beam-detector pair has a different geometry but defines *exactly* the same scattering vector (in direction as well as magnitude). Thus, for single scattering the arrangement is degenerate in that each detector observes exactly the same spatial Fourier component of the sample. It is simple to show [4], however, that for double and higher-order multiple scattering this degeneracy is broken. Then each detector observes several *different* Fourier components. Different spatial Fourier components of a sample are statistically independent, i.e., their temporal fluctuations are uncorrelated. Thus, when the two scattered intensities (each comprising single and multiple scattering) are cross correlated, nontrivial correlations are observed only between the singly scattered parts. The net result is that the time-dependent part of the measured time cross-correlation function of the scattered intensities reflects single scattering alone; multiple scattering contributes only to the time-independent ''background.'' As mentioned above, emphasis hitherto has been on studying the *dynamics* of turbid samples by this method. Here we exploit the fact that the amplitude of the time-dependent part of the cross-correlation function, relative to the background, is related to the ratio of single to total scattering by the sample, thus allowing accurate *static* light scattering on turbid samples.

Two schemes for multiple-scattering suppression, both originally proposed by Schätzel [4], have emerged as favorites. In two-color dynamic light scattering (TCDLS) [4–7], the incident and scattered beams all lie in the same scattering plane. Laser beams of two different colors, usually the blue (B), wavelength *in vacuo* $\lambda_{B,0}=488$ nm, and green (G), $\lambda_{G,0}=514.5$ nm, lines of an argon ion laser, are focused into the sample at small crossing angle 2α. Detectors, also separated by angle 2α, are set at average scattering angle θ, each detecting light of one or the other color. The green light is scattered through the larger angle $\theta+2\alpha$, whereas the scattering angle for the blue light is $\theta-2\alpha$. It is straightforward to show that, when θ and α satisfy the relationship

$$\tan\alpha=\left(\frac{\lambda_G-\lambda_B}{\lambda_G+\lambda_B}\right)\tan\left(\frac{\theta}{2}\right), \tag{2}$$

the scattering vectors for blue and green scattered light are the same [4]. Segrè *et al.* [7] have given a detailed description of TCDLS equipment and its use.

In the second method, three-dimensional dynamic light scattering [4,8–11], two light beams of the same color enter the sample from slightly above and slightly below the average scattering plane, and detectors at scattering angle θ are similarly placed above and below the plane. In this case the degenerate pairs that define the same scattering vector are the incident beam entering the sample from below the average scattering plane and the detected beam above the plane and *vice versa*.

Each method has its advantages and disadvantages. In TCDLS the use of narrow-band optical filters ensures that each detector ''sees'' scattered light of only one color. Then, for a *single*-scattering sample, the amplitude of the time-dependent part of the measured intensity cross-correlation function (relative to its ''background'') is nearly as large as for the case when scattered light of one color is autocorrelated. By contrast, in the three-dimensional method *both* detectors see scattered light from *both* incident beams; then, even for single scattering, the relative amplitude of the time-dependent part of the cross-correlation function is reduced by a factor of 4 compared to the autocorrelation function. On the other hand, after initial alignment, the three-dimensional equipment is robust, requiring only one operation to alter the scattering angle, the motion of the arm carrying the two detectors. In TCDLS, not only must the detector arm be moved to change the average scattering angle θ, but the crossing angle 2α of both incident and scattered beams must also be altered; further minor adjustments are frequently necessary to maximize the amplitude of the cross correlation.

In this work we use the two-color equipment. We mention, however, that the application of cross-correlation, multiple-scattering suppression, schemes to static (as well as dynamic) light scattering has been developed by others [9,10] besides ourselves [2,3]. This other work used the three-dimensional method and emphasized the measurement of particle form factors in turbid but still quite dilute samples. Here we describe the determination of structure in concentrated samples.

II. THEORY

The photon correlator used in ordinary dynamic light scattering usually gives as its output the normalized time autocorrelation function $g_A^{(2)}(Q,\tau)$ of the scattered intensity $I(Q,t)$. For single-scattering samples, $g_A^{(2)}(Q,\tau)$ is related to the normalized intermediate scattering function $f(Q,\tau)$ of the sample by

$$g_A^{(2)}(Q,\tau)\equiv\frac{\langle I(Q,0)I(Q,\tau)\rangle}{\langle I(Q)\rangle^2}=1+\beta^2[f(Q,\tau)]^2, \tag{3}$$

where the angle brackets indicate a time average. (In this paper we consider only fluidlike, *ergodic* samples, so that time and ensemble averages are equivalent.) The intermediate scattering function is the time autocorrelation function of the Qth spatial Fourier component of the refractive-index fluctuations of the sample and provides information on the sample's dynamics; $f(Q,\tau)$ can also be interpreted as the normalized autocorrelation function of the amplitude of the singly scattered electric field. The intermediate scattering function for an ergodic medium has the limits

$$\lim_{\tau\to 0} f(Q,\tau)=1, \quad \lim_{\tau\to\infty} f(Q,\tau)=0. \tag{4}$$

In Eq. (3) β is a parameter slightly smaller than 1, determined by the ratio of the size of the detector apertures to the size of the coherence areas of the scattered light.

Two-color dynamic light scattering measures the time *cross*-correlation function $g_C^{(2)}(Q,\tau)$ of the intensities $I_{B,G}(Q,t)$ of scattered light of the two colors. This function is given by (see [7] for details)

$$g_C^{(2)}(Q,\tau)\equiv\frac{\langle I_B(Q,0)I_G(Q,\tau)\rangle}{\langle I_B(Q)\rangle\langle I_G(Q)\rangle}=1+\beta^2\beta_{\rm OV}^2\beta_{\rm MS}^2[f(Q,\tau)]^2. \tag{5}$$

Compared to Eq. (3), two new parameters, $\beta_{\rm OV}$ and $\beta_{\rm MS}$, appear in Eq. (5). The ''overlap factor'' $\beta_{\rm OV}$, generally slightly smaller than 1, accounts for the fact that the scattering volumes seen by the two detectors are slightly different. The ''multiple scattering factor'' $\beta_{\rm MS}$ is the quantity of interest in this work since it is related to the ratios of the average intensities of singly scattered light $\langle I_{B,G}^S(Q)\rangle$ to total (single + multiple) scattered light $\langle I_{B,G}(Q)\rangle$ by [7]

$$\beta_{\rm MS}^2(Q)=\frac{\langle I_B^S(Q)\rangle}{\langle I_B(Q)\rangle}\frac{\langle I_G^S(Q)\rangle}{\langle I_G(Q)\rangle}. \tag{6}$$

By writing $\beta_{\rm MS}=\beta_{\rm MS}(Q)$, we emphasize its (often strong) dependence on scattering vector Q. For a single-scattering sample, $\beta_{\rm MS}(Q)=1$, since the single and total scattered intensities are the same.

Equations (5) and (6) quantify the statements made in Sec. I. First we note that the time dependence of $g_C^{(2)}(Q,\tau)$ is determined solely by $f(Q,\tau)$, which reflects just single scattering; this is the property exploited when TCDLS is used to study dynamics. Multiple scattering contributes only to the time-independent background of the intensity cross-correlation function. Thus its effect on the *normalized* function $g_C^{(2)}(Q,\tau)$ is simply to reduce the amplitude of the time-dependent term, the magnitude of this reduction being expressed by the value of $\beta_{\rm MS}$.

In this work we make a quantitative measurement of $\beta_{\rm MS}(Q)$ and use it to correct for multiple scattering in static light scattering. The zero-time limits of Eqs. (4) and (5) give

$$g_C^{(2)}(Q,0)=1+\beta^2\beta_{\rm OV}^2\beta_{\rm MS}^2. \tag{7}$$

We obtain $\beta_{\rm MS}^2(Q)$ as follows. At each value of Q we first measure $g_C^{(2)}(Q,0)$ by TCDLS for the turbid sample of interest. Then we repeat the measurement, under exactly the same experimental conditions, so that β and $\beta_{\rm OV}$ remain the same for a dilute ''reference'' sample that shows no multiple scattering and so that $\beta_{\rm MS}(Q)=1$. The ratio of the two values of $g_C^{(2)}(Q,0)-1$ then gives $\beta_{\rm MS}^2(Q)$ directly [see Eq. (7)].

The analysis proceeds as follows. From Eq. (6) we have

$$\langle I_B^S(Q)\rangle\langle I_G^S(Q)\rangle=\beta_{\mathrm{MS}}^2(Q)\langle I_B(Q)\rangle\langle I_G(Q)\rangle. \tag{8}$$

Thus multiplying the product of the detected total scattered intensities by $\beta_{\mathrm{MS}}^2(Q)$, measured as described above, effectively removes multiple scattering and leaves the product of the detected single-scattered intensities.

A second effect of strong scattering by a turbid sample, namely, attenuation, must also be accounted for. On propagation of an illuminating laser beam through the sample the number of unscattered photons is reduced by scattering out of the beam. The singly scattered light, propagating from the scattering volume to the detector, is similarly attenuated. Thus although $\langle I_B^S(Q)\rangle$ and $\langle I_G^S(Q)\rangle$ [Eq. (8)] reflect only single-scattered photons, there are fewer of these than there would be without attenuation. In our experiments, the sample is contained in a cylindrical cell and a small scattering volume is selected on the axis of the cylinder. Thus, on propagating from the scattering volume to the detector, the singly scattered light is attenuated by the same fraction as the direct laser beam on propagating from the center of the cell to the wall. Therefore the fractional reduction of the number of singly scattered photons caused by attenuation is the same as the fractional reduction of the intensity of the direct laser beam on passage through the whole sample. We define the sample's transmission $T_{B,G}$ as the ratio of the intensity of the direct (blue/green) laser beam transmitted through the sample to that incident on it. These transmissions can be measured easily and quickly. Then we can obtain the product of single-scattered intensities $\langle I_B^S(Q)\rangle_0\langle I_G^S(Q)\rangle_0$, corrected for both multiple scattering and attenuation, from

$$\langle I_B^S(Q)\rangle_0\langle I_G^S(Q)\rangle_0=\frac{\langle I_B^S(Q)\rangle}{T_B}\frac{\langle I_G^S(Q)\rangle}{T_G}=\beta_{\mathrm{MS}}^2(Q)\frac{\langle I_B(Q)\rangle}{T_B}\frac{\langle I_G(Q)\rangle}{T_G}. \tag{9}$$

The corrected intensity scattered by a concentrated suspension of spherical colloidal particles can be written [12]

$$\langle I_{B,G}^S(Q)\rangle_{0,\mathrm{conc}}=I_{0,B,G}C_{\mathrm{conc}}K_{B,G}P(Q)S(Q). \tag{10}$$

Here $I_{0,B,G}$ are the incident laser intensities, C_{conc} is the concentration of the sample, $K_{B,G}$ are (wavelength-dependent) constants of proportionality, and $P(Q)$ and $S(Q)$ are, respectively, the form factor of particles and the structure factor of the sample. [For polydisperse particles, $P(Q)$ is the average form factor and $S(Q)$ is the ''measured'' structure factor [12].] For a sample dilute enough that $S(Q)=1$, the analogous result is

$$\langle I_{B,G}^S(Q)\rangle_{0,\mathrm{dil}}=I_{0,B,G}C_{\mathrm{dil}}K_{B,G}P(Q). \tag{11}$$

From Eqs. (10) and (11) we get an expression for the structure factor

$$S(Q)=\left[\frac{\langle I_B^S(Q)\rangle_{0,\mathrm{conc}}\langle I_G^S(Q)\rangle_{0,\mathrm{conc}}}{\langle I_B^S(Q)\rangle_{0,\mathrm{dil}}\langle I_G^S(Q)\rangle_{0,\mathrm{dil}}}\right]^{1/2}\frac{C_{\mathrm{dil}}}{C_{\mathrm{conc}}}. \tag{12}$$

Substitution of Eq. (9) in Eq. (12) then gives the structure factor in terms of the basic measured quantities:

$$S(Q)=\left[\frac{\langle I_B(Q)\rangle_{\mathrm{conc}}\langle I_G(Q)\rangle_{\mathrm{conc}}}{\langle I_B(Q)\rangle_{\mathrm{dil}}\langle I_G(Q)\rangle_{\mathrm{dil}}}\right]^{1/2}\times\frac{C_{\mathrm{dil}}}{C_{\mathrm{conc}}}\left[\frac{T_{B,\mathrm{dil}}}{T_{B,\mathrm{conc}}}\frac{T_{G,\mathrm{dil}}}{T_{G,\mathrm{conc}}}\right]^{1/2}\frac{\beta_{\mathrm{MS,conc}}(Q)}{\beta_{\mathrm{MS,dil}}(Q)}. \tag{13}$$

In our early work we used a slightly simpler approach by assuming that the wavelengths of green and blue light are close enough that the ratios of single and total scattered light are the same for both colors; i.e.,

$$\frac{\langle I_B^S(Q)\rangle}{\langle I_B(Q)\rangle}=\frac{\langle I_G^S(Q)\rangle}{\langle I_G(Q)\rangle}, \tag{14}$$

so that, from Eq. (6),

$$\beta_{\mathrm{MS}}(Q)=\frac{\langle I_B^S(Q)\rangle}{\langle I_B(Q)\rangle}=\frac{\langle I_G^S(Q)\rangle}{\langle I_G(Q)\rangle}. \tag{15}$$

Then for one color, say green, we have

$$\langle I_G^S(Q)\rangle=\beta_{\mathrm{MS}}(Q)\langle I_G(Q)\rangle. \tag{16}$$

The result analogous to Eq. (12) is then

$$S(Q)=\frac{\langle I_G^S(Q)\rangle_{0,\mathrm{conc}}}{\langle I_G^S(Q)\rangle_{0,\mathrm{dil}}}\frac{C_{\mathrm{dil}}}{C_{\mathrm{conc}}}, \tag{17}$$

where

$$\langle I_G^S(Q)\rangle_0=\frac{\langle I_G^S(Q)\rangle}{T_G}=\frac{\beta_{\mathrm{MS}}(Q)\langle I_G(Q)\rangle}{T_G}. \tag{18}$$

III. EXPERIMENT

A. The samples

We used the same type of colloidal particles as in previous work [12] comprising ''cores'' of poly(methylmethacrylate) (PMMA) stabilized sterically by chemically grafted layers of poly-12-hydroxystearic acid (PHSA). We estimate the refractive index of the composite particles to be about 1.492. The particles were dispersed in pure *cis*-decahydronaphthalene (decalin), having refractive index 1.481. The samples were contained in thick-walled cylindrical tubes with inner diameter 2 mm, the short light path being used to minimize the effect of multiple scattering. The particles used for the structure factor measurements had hydrodynamic radius $R_H=217\pm3$ nm and a polydispersity of 0.045 ± 0.01, as measured by (two-color) dynamic light scattering on a dilute sample [13]. Particle volume fractions ϕ were determined as follows. The ''core'' volume fraction of a stock suspension was calculated from measured weights of *cis*-decalin and dry particles, using literature values for the densities ($\rho_p=1.18$ gm cm^{-3} for PMMA particles; $\rho_s=0.896$ gm cm^{-3} for *cis*-decalin). Samples at other concentrations were prepared from the stock suspension by the addition or removal (after centrifuging) of liquid. Core volume fractions were then converted to their ''hard-sphere'' values ϕ, by

multiplication by a scaling factor such that the concentration of a sample at the thermodynamic freezing transition (i.e., where the formation of colloidal crystals was first observed) had the computer value $\phi = 0.494$ [14]. This scaling factor, 1.185 in this case, allows for the fact that the thermodynamic volume of a particle is larger than the core volume because of solvation of the 10–15 nm stabilizing layer of PHSA [15]. We estimate the uncertainty in ϕ to be less than 1% at $\phi \sim 0.50$ and to be no more than 2% at lower concentrations.

The dilute ''reference'' sample, used to measure the amplitude of the intensity cross-correlation function in the absence of multiple scattering (see Sec. II), comprised similar particles of radius 115 nm also dispersed in *cis*-decalin. This small size was chosen so that the minimum of the particle's form factor lies outside the range of scattering angle used, ensuring reasonably strong single scattering at all angles. The reference sample was prepared at a concentration large enough that the scattering from the particles dominated that of the liquid, but low enough that there was negligible multiple scattering. Its transmission was about 95%.

B. Light scattering

The two-color dynamic light-scattering equipment was manufactured by ALV, Langen, Germany, and has been described in detail in [7]. Two argon ion lasers provided the blue and green light. These were run in a ''light control'' mode at nominal powers of about 50 mW. The powers were checked regularly with a power meter, and did not vary by more than 1% during the measurements. The samples were contained in a cylindrical bath filled with toluene that nearly matched the refractive index of the scattering cell. The intensities of blue and green light transmitted through the bath when it contained samples were measured by the power meter. The ratio of the intensity transmitted when the bath contained the sample of interest to that transmitted when the bath contained a sample tube of pure decalin gave the sample's transmission T. The uncertainty in the measurement of transmission was estimated to be about 2%.

Though tedious and time consuming, the light-scattering measurements were relatively straightforward. At each scattering angle θ the singly scattering reference sample was studied first. As described elsewhere [7], fine adjustments were made of the beam positions and directions and of the beam crossing angles α in both the illuminating and detection arms of the equipment to give the maximum value of the cross-correlation amplitude $g_C^{(2)}(Q,0)(=1+\beta^2\beta_{\mathrm{OV}}^2)$. This ensured optimum alignment of the equipment. Then the sample of interest was placed in the equipment and five experiments, each of 5 min duration, were performed to measure the cross-correlation amplitude, $g_C^{(2)}(Q,0)(=1+\beta^2\beta_{\mathrm{OV}}^2\beta_{\mathrm{MS}}^2)$ and the total scattered intensities $\langle I_{B,G}(Q)\rangle$. Finally the reference sample was returned to the equipment to check that the alignment of the equipment, was still optimum. This whole procedure was then repeated at a new scattering angle. The uncertainties in the measurements of $g_C^{(2)}(Q,0)-1$ and $\langle I_{B,G}(Q)\rangle$ were about 2% and 1%, respectively. Combining the uncertainties in all the measured quantities on the right-hand side of Eq. (13), we estimate that structure factors can be measured by this method to an accuracy of about $\pm 5\%$.

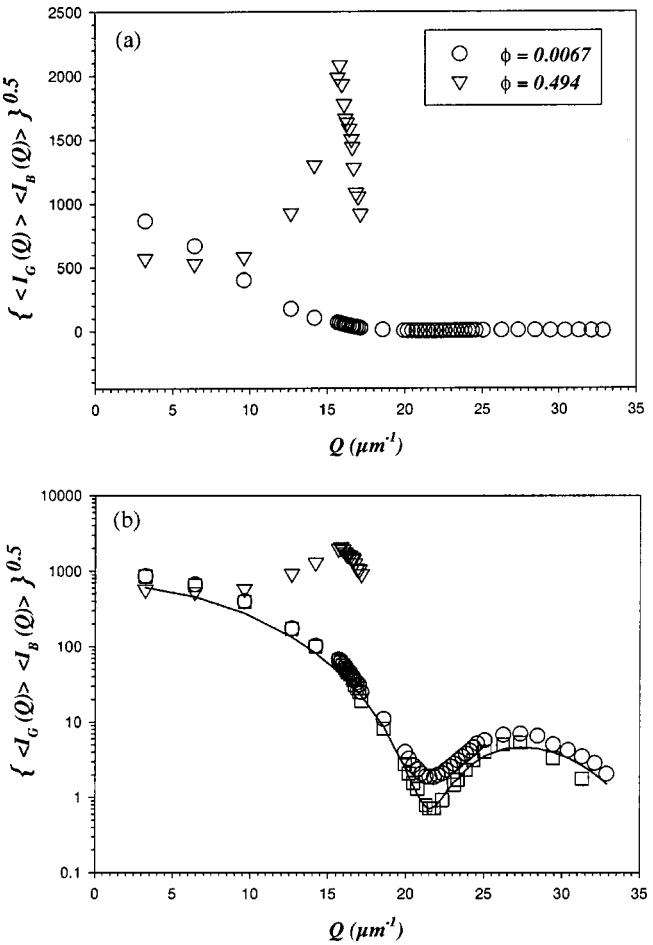

FIG. 1. (a) Dependence on the scattering vector of the total intensities scattered by suspensions of PMMA particles in *cis*-decalin at volume fractions $\phi = 0.0067$ and 0.494. The ordinate is the square root of the product of the intensities of blue and green scattered light, corrected for the dependence of scattering volume on scattering angle (see text). (b) The same data replotted with a logarithmic ordinate axis. The squares show the data for the dilute sample after correction for multiple scattering (see text). The solid line is the average form factor of homogeneous spheres with mean radius $R = 208$ nm and polydispersity 0.046. In both (a) and (b) the units of intensity are 1000 counts/s.

IV. RESULTS AND DISCUSSION

Figure 1 shows the dependence on the scattering vector of the geometric means of the intensities of the total scattering of blue and green light for the PMMA samples, described in Sec. III A, at volume fractions $\phi = 0.0067$ and $\phi = 0.494$. The blue and green intensities have been multiplied by the factors $\sin(\theta - 2\alpha)$ and $\sin(\theta + 2\alpha)$, respectively, to allow for the angle dependence of the scattering volumes. The data for the dilute sample reflect largely the form factor of homogeneous spheres (discussed further below). Despite strong multiple scattering (see below), the effect of the main peak in the structure factor of the concentrated sample is clearly evident in the data of Fig. 1. We now consider, in sequence, the effects of the various factors on the right-hand side of Eq. (13) when the structure factor $S(Q)$ is calculated from the ''raw'' data of Fig. 1.

In Figure 2 the diamonds show the first two factors of Eq. (13), the product of the ratio of the scattered intensities, and

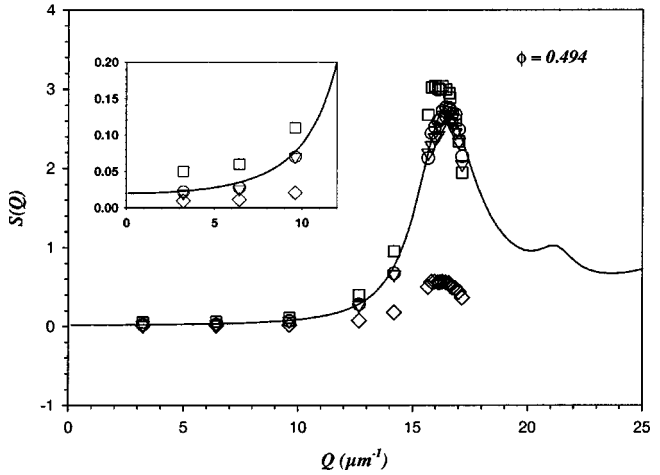

FIG. 2. Various estimates of the structure factor of a supension of PMMA particles at volume fraction $\phi=0.494$ (see text for detailed discussion). Diamonds, the simplest estimate, totally ignoring multiple scattering. The data of Fig. 1 for $\phi=0.494$ divided by the data for $\phi=0.0067$ and multiplied by the concentration ratio [the first two factors on the right-hand side of Eq. (13)]. Squares, correction for attenuation. The data represented by diamonds, multiplied by the ratio of sample transmissions [i.e., the first three factors of Eq. (13)]. Circles, correction for multiple scattering. The result of applying all factors in Eq. (13). Inverted triangles, fully corrected data obtained using the simpler procedure described in Sec. II. The solid line is the theoretical structure factor for hard spheres at volume fraction $\phi=0.494$ and polydispersity 0.046 in the Percus-Yevick approximation.

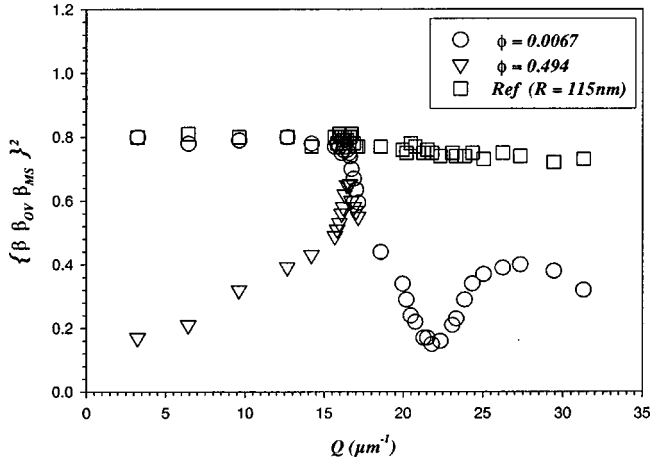

FIG. 3. Amplitudes of the measured intensity cross-correlation functions, $g_C^{(2)}(Q,0)-1=\beta^2\beta_{\rm OV}^2\beta_{\rm MS}^2$, as functions of the scattering vector for three samples. Squares, the reference, single-scattering sample for which $\beta_{\rm MS}=1$. The slight drop of the amplitude for this sample at large Q results from increasingly incomplete overlap of the two scattering volumes, described by $\beta_{\rm OV}$. Circles, the dilute sample at $\phi=0.0067$. The reduced amplitude around $Q=22\ \mu{\rm m}^{-1}$ indicates significant multiple scattering near the minimum of the particles' form factor. Inverted triangles, the concentrated sample at $\phi=0.494$.

the ratio of the concentrations (or volume fractions) for the two samples. If neither sample showed any multiple scattering, this product would yield the structure factor directly [since, in Eq. (13), both the transmissions T and the multiple-scattering factors $\beta_{\rm MS}$ would be 1]. While the results of this operation have the general shape expected for the structure factor of hard spheres their absolute magnitudes are much too low, by a factor of up to ~ 5. Next we multiply these results by the ratios of transmissions (measured to be $T_{B,\rm conc}=0.178$, $T_{B,\rm dil}=0.878$, $T_{G,\rm conc}=0.177$, and $T_{G,\rm dil}=0.871$), the third factor in Eq. (13). This product of the first three terms in Eq. (13) is represented by the squares in Fig. 2. At first sight, these results look similar to the theoretically predicted structure factor (the solid line in Fig. 2; see below). However, closer inspection shows that, at least up to the main peak, their values are all larger; as shown in the inset of Fig. 2, the difference is about a factor of 2 at small Q.

Now we make the correction for multiple scattering. Figure 3 shows the product $\beta^2\beta_{\rm OV}^2\beta_{\rm MS}^2$, obtained from the measured values of $g_C^{(2)}(Q,0)-1$ [Eq. (7)], for three samples. For the ''reference'' sample, a dilute suspension of small spheres (see Sec. III A), multiple scattering is negligible, so that $\beta_{\rm MS}=1$. Thus the data in Fig. 3 just represent $\beta^2\beta_{\rm OV}^2$, accounting for the finite size of the detector apertures and the incomplete overlap of the two scattering volumes (Sec. II). We see that this quantity has a value of about 0.8 at low Q, dropping somewhat at higher Q due, probably, to decreased overlap of the scattering volumes as the crossing angle α is increased (see Sec. I and [7]). For the dilute sample ($\phi=0.0067$), $\beta^2\beta_{\rm OV}^2\beta_{\rm MS}^2$ has values similar to those of the reference sample at low Q, implying relatively little multiple scattering. However, at higher Q the values drop in the region of the minimum in the particle form factor, indicating some multiple scattering. For the concentrated sample ($\phi=0.494$), $\beta^2\beta_{\rm OV}^2\beta_{\rm MS}^2$ is small at low Q, implying significant multiple scattering, but larger near the structure factor peak where the single scattering becomes strong. The values of $\beta_{\rm MS}^2$ are obtained by dividing the values of $\beta^2\beta_{\rm OV}^2\beta_{\rm MS}^2$, shown in Fig. 3, for the sample of interest by those for the reference sample for which $\beta_{\rm MS}=1$. Thus, at low Q, $\beta^2\beta_{\rm OV}^2\beta_{\rm MS}^2\approx 0.16$ for the concentrated sample and ≈ 0.80 for the test sample, giving $\beta_{\rm MS}^2\approx 0.20$ and $\beta_{\rm MS}\approx 0.45$. From Eq. (6) this implies that single scattering constitutes about 45% of the total scattering.

The circles in Fig. 2 represent the structure factor $S(Q)$ of the concentrated sample obtained from the full Eq. (13), i.e., including the final factor that effectively removes the multiple scattering. The solid line is the theoretical structure factor calculated from the Percus-Yevick approximation for hard spheres with a polydispersity of 0.046 [16], incorporating the Verlet-Weis correction [17] to the volume fraction, i.e., $\phi\rightarrow\phi-\phi^2/16$. [In this calculation we used a number-average radius of $R=214$ nm, calculated from $R=R_H/(1+5\sigma^2)$, where σ is the polydispersity [13].] As discussed in Sec. III B, we estimate the uncertainty in the measured structure factor to be about $\pm 5\%$, i.e., slightly larger than the data symbols near the peak of $S(Q)$ and significantly smaller at low Q (inset of Fig. 2). Overall there is remarkably good agreement between experiment and theory, even at small Q where the multiple scattering is strong. The experimental data become inaccurate for $QR\geqslant 3.5$ as the minimum of the particle form factor at $QR=4.49$ is approached.

As discussed in Sec. II, strong scattering by the sample has two distinct effects in static light scattering. First, the detector ''sees'' both singly and multiply scattered light.

Second, the singly scattered light is attenuated by the scattering of photons out of both the illuminating and scattered beams. The step-by-step data analysis given in the previous paragraphs shows that, perhaps surprisingly, the effect of attenuation on the raw data appears to be much greater than the effect of detecting multiply scattered light. A close look at the small-Q data, however, shows that both corrections are necessary to get the correct structure factor (inset of Fig. 2). The uncorrected estimates, the diamonds in Fig. 2, give values of $S(Q)$ too small by a factor of ~ 2 at small Q. Correction for just attenuation, the squares in Fig. 2, overestimates $S(Q)$, also by a factor of ~ 2. Only when the additional correction for multiple scattering is made is good agreement found between experiment and theory. Since $\lim_{Q\to 0} S(Q)$ contains valuable information about the sample — it is proportional to the osmotic compressibility — this is not a trivial point.

The inverted triangles in Fig. 2 show the structure factor for the concentrated sample, $\phi = 0.494$, estimated by the simpler method outlined in Sec. II where the ratios of single- to multiple-scattered light are assumed to be the same for both colors and light of only one color, green in this case, is used in the calculation [see Eqs. (14)–(18)]. These results agree, to within estimated uncertainties, with those, the circles, obtained by the more complete method, implying that, for these samples at least, Eq. (14) must be reasonably accurate.

For clarity, Fig. 4(a) replots the fully corrected data of Fig. 2 for $\phi = 0.494$. Figures 4(b) and 4(c) show structure factors of samples of the same particles at lower concentrations $\phi = 0.426$ and $\phi = 0.366$, measured by the simpler method and compared with theory. Again agreement is good, except perhaps for a couple of data points at $\phi = 0.366$ that lie at the limit of experimental uncertainty. We mention that, in practice, there is little reason not to use the more complete method, Eqs. (8)–(13). During the measurement of β_{MS}, Eq. (7), the photon correlator automatically stores both the total scattered intensities $\langle I_B(Q)\rangle$ and $\langle I_G(Q)\rangle$. Thus the only extra information needed to apply Eqs. (8)–(13) is the easily measured transmission of the sample at the second color.

Finally we return to the data for the dilute sample, $\phi = 0.0067$, shown in Fig. 1(b). The results of Fig. 3 show that, although dilute, this sample still exhibits significant multiple scattering near the minimum in its form factor at $Q \approx 22\ \mu\mathrm{m}^{-1}$ where the single scattering is weak: the measured values of $\beta^2\beta_{\mathrm{OV}}^2\beta_{\mathrm{MS}}^2$ are significantly lower than those for the reference sample. The results of correcting these data for multiple scattering, as described above, are shown as the squares in Fig. 1(b). At small Q, there is little difference between corrected and uncorrected results. However, removal of the multiple scattering has a marked effect at and beyond the form factor minimum; in particular it reveals a deeper minimum at $Q_{min} = 21.6\ \mu\mathrm{m}^{-1}$. If we assume the particles to be homogeneous, this yields a particle radius, $4.49/Q_{min} = 208$ nm. [That this value of radius is somewhat smaller than that, 214 nm, obtained from dynamic light scattering (above), implies that, when calculating the form factor, it is strictly necessary to take account of the fact that the core and stabilizing layer of the particle have different refractive indices.] The line in Fig. 1(b) shows a calculated form factor for homogeneous particles with average radius $R = 208$ nm and polydispersity 0.046. In the region of the form factor minimum this calculated result fits the data well; the value of polydispersity also agrees well with that, 0.046 ± 0.01, obtained from dynamic light scattering (Sec. III A). The suppression of multiple scattering in the measurement of form factors is also described in Refs. [9,10].

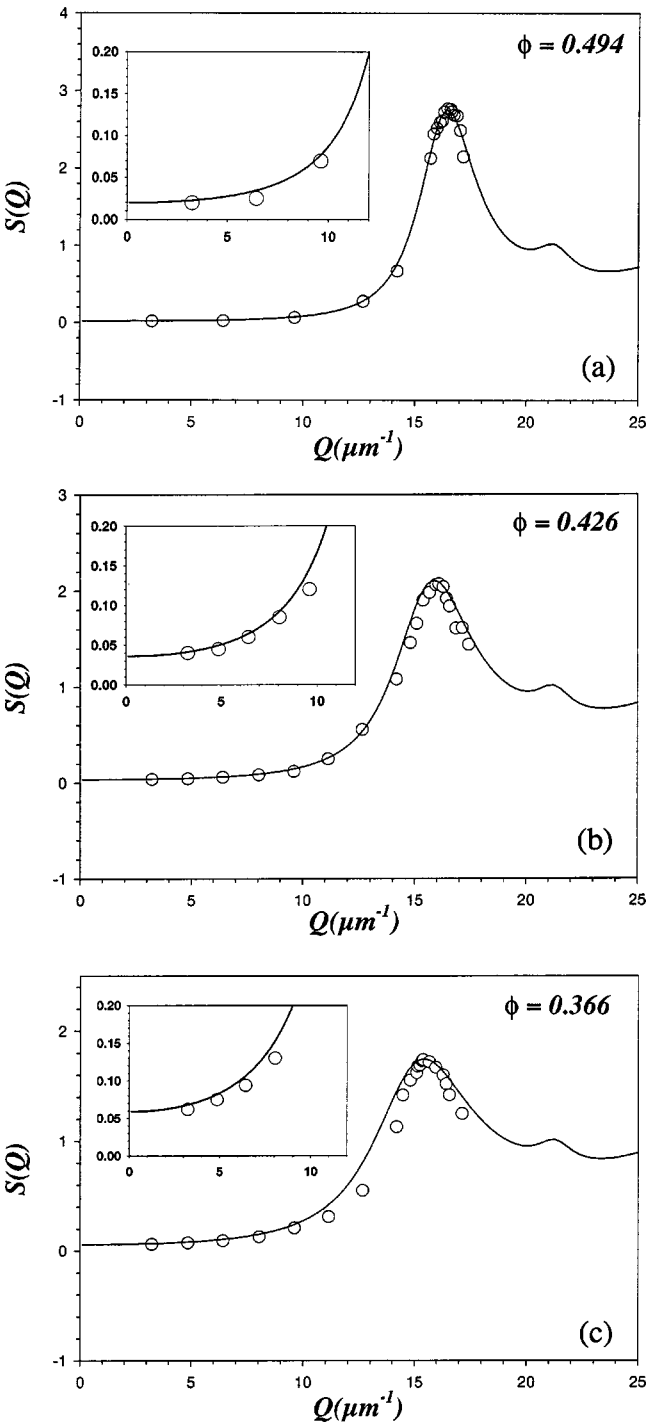

FIG. 4. Fully corrected structure factor of Fig. 2 replotted for clarity and compared with the theoretical Percus-Yevick prediction. (b), (c). Similar results for $\phi = 0.426$ and 0.366. The results of (a) were obtained using the complete method represented by Eqs. (8)–(13), whereas those of (b) and (c) used the simpler method, Eqs. (14)–(17), in which the ratio of single to total scattering is assumed to be the same for blue and green light (see text for further discussion).

V. CONCLUDING REMARKS

Previously the main approach used to measure the structure of concentrated suspensions by light scattering has been refractive-index matching [18]. Here the particles are suspended in a liquid, or more usually a mixture of liquids, whose refractive index is very close to that of the particles, thus reducing the sample's scattering power to the point where multiple scattering is negligible. This method is fraught with difficulties. The weak single scattering can be corrupted by scattering from cell walls and from dust, which is very difficult to remove completely from concentrated suspensions. More important, difficulties stem from the fact that sterically stabilized particles are typically composed of a core and a shell having different refractive indices. Near to index-match, interference between the light scattered by the core and that scattered by the shell leads to particle form factors that can vary strongly with suspension conditions (particularly with the refractive index of the suspension medium) and can be difficult to control [18,19]. Furthermore, index matching and the particle's core-shell structure interact in a rather subtle way to magnify greatly the effect of the sample's polydispersity on the measured structure factor [20].

In this paper we have shown how the two-color dynamic light-scattering method, used hitherto to study the dynamics of turbid samples, can also be exploited to suppress multiple scattering in static light scattering. Then turbid samples can be studied significantly away from refractive-index matching. The strong single scattering dominates scattering by dust and cell walls and the multiple scattering is suppressed. The other difficulties (above) associated with index matching are also circumvented. We have illustrated the method by measuring structure factors of suspensions of hard-sphere colloids. Very good agreement between the experimental results and Percus-Yevick theory for the structure factors of hard spheres is found. For the reasons just given, these are probably the most accurate light-scattering measurements on such systems to date. Finally we mention that elsewhere [2,3] we have reported measurements by this technique of the structure factors of the ''colloidal liquid'' phases of colloid-polymer mixtures, as a function of the range of the ''depletion potential'' induced by the polymer. As the range of the potential becomes smaller, accurate measurements of the liquids' structure factors at small Q indicate increasingly large long-ranged density fluctuations.

ACKNOWLEDGMENTS

The work reported here was supported by the Biotechnology and Biological Sciences Research Council (Grant No. E04113). We thank Bruno D'Aguanno for the polydisperse hard-sphere (Percus-Yevick) program. We also thank Wilson Poon for valuable discussions and for reading the manuscript. The particles used in this work were made by Debbie Stokes.

[1] G.D.J. Phillies, J. Chem. Phys. **74**, 260 (1981); Phys. Rev. A **24**, 1939 (1981).
[2] P.N. Pusey, P.N. Segrè, W.C.K. Poon, S.P. Meeker, O.P. Behrend, and A. Moussaïd, in *Modern Aspects of Colloidal Dispersions*, edited by R.H. Ottewill and A.R. Rennie (Kluwer, Dordrecht, 1998).
[3] A. Moussaïd, W.C.K. Poon, P.N. Pusey, and M.F. Soliva, Phys. Rev. Lett. **82**, 225 (1999).
[4] K. Schätzel, J. Mod. Opt. **38**, 1849 (1991).
[5] K. Schätzel, M. Drewel, and J. Ahrens, J. Phys.: Condens. Matter **2**, SA393 (1990).
[6] M. Drewel, J. Ahrens, and U. Podschus, J. Opt. Soc. Am. A **7**, 206 (1990).
[7] P.N. Segrè, W. van Megen, P.N. Pusey, K. Schätzel, and W. Peters, J. Mod. Opt. **42**, 1929 (1995).
[8] E. Overbeck, C. Sinn, T. Palberg, and K. Schätzel, Colloids Surf., A **122**, 83 (1997).
[9] L.B. Aberle, P. Hulstede, S. Wiegand, W. Schroer, and W. Staude, Appl. Opt. **37**, 6511 (1998).
[10] C. Urban and P. Schurtenberger, J. Colloid Interface Sci. **207**, 150 (1998).
[11] E. Overbeck and C. Sinn, J. Mod. Opt. **46**, 303 (1999).
[12] See, for example, P.N. Pusey, in *Liquids, Freezing and the Glass Transition*, Les Houches Session LI, edited by D. Levesque, J.-P. Hansen, and J. Zinn-Justin (North-Holland, Amsterdam, 1991), pp. 763–942.
[13] P.N. Pusey and W. van Megen, J. Chem. Phys. **80**, 3513 (1984).
[14] W.G. Hoover and F.H. Ree, J. Chem. Phys. **49**, 3609 (1968).
[15] P.N. Pusey and W. van Megen, Nature (London) **320**, 340 (1986).
[16] P. van Beurten and A. Vrij, J. Chem. Phys. **74**, 2744 (1981).
[17] L. Verlet and J.J. Weis, Phys. Rev. A **5**, 939 (1972).
[18] W. van Megen and P.N. Pusey, Phys. Rev. A **43**, 5429 (1991).
[19] I. Markovic and R.H. Ottewill, Colloid Polym. Sci. **264**, 65 (1986); I. Livsey and R.H. Ottewill, Adv. Colloid Interface Sci. **36**, 173 (1991).
[20] Y.D. Yan and J.H.R. Clarke, J. Chem. Phys. **93**, 4501 (1990); J. Ricka, M. Borkovec, and U. Hofmeier, *ibid.* **94**, 8503 (1991).